

**Final Report to the Office of Naval Research  
Contract N0014-94-1-0834**

**Dr. Geoffrey L. Main  
Program Manager, Code 1222**

**Dr. Jerry H. Ginsberg  
Principal Investigator  
G. W. Woodruff Chair  
School of Mechanical Engineering  
Georgia Institute of Technology  
Atlanta, GA 30332-0405**

**Submitted December 15, 1994**

This document has been approved  
for release and sale; its  
distribution is unlimited.

19941219 043

## 1. Overview

The task of modeling the shock response of submerged structures has always been implemented in the time domain, in contrast to the frequency domain approach used for structural acoustic modeling of radiation and scattering. One approach used to create time domain representations of the interaction of the structure and surrounding fluid is to develop a finite element simulation in which a large domain of the fluid is included in the mesh. Because this procedure leads to a very large model that strains available computer resources, it limits the fidelity with which the structure may be modeled. For this reason approximate procedures that replace the fluid with an impedance-type condition have been derived. Of these, the most widely implemented is the doubly-asymptotic approximation (DAA), which has been developed in a variety of versions. The original derivation of DAA by Geers was achieved by analysis of the behavior of spheres [1] and infinitely long cylinders [2]. With only two exceptions, analytical validation efforts have continued to consider these geometries only. The exceptions are a study by Wawa and DiMaggio [3], which employed finite differences to check DAA for a slightly eccentric prolate spheroidal shell, and a work by Olson and Bathe [4], which employed DAA as the basis for an infinite element to be applied away from the wetted surface. The unavailability of analytical solutions for slender bodies makes it impossible to examine analytically the quality of time-domain DAA. There has been a large number of validation studies assessing the technique in comparison to experiments at various scale. The results of such work have been inconsistent, with some indicating excellent agreement and others indicating significant differences. To some extent these discrepancies can be explained by differences in the selection of the DAA version and the adequacy of the model. However, in the absence of analytical capabilities, prior to the initiation of the present project there were no existing guidelines identifying the overall limitations of DAA in realistic configurations, and the spatial and temporal scales where its application should be avoided.

The research project began to address this shortcoming. The fundamental concept driving the research was conversion of the time domain model to an equivalent frequency domain form. The basis for this work was an analysis by Nicholas-Vuillierme [5] that converted the temporal differential equations associated with DAA to equivalent algebraic equations relating the surface pressure and normal velocity distributions at specified frequency. It is reasonable to examine the frequency domain behavior of DAA because even the relatively short duration

A-1

of a large, close explosive source leads to a signal whose primary amplitude and energy content is in the frequency range  $ka < 10$ .

The methodology followed in the proposal was to use a standard frequency domain technique to derive an alternative surface impedance matrix giving the surface pressure associated with a specified velocity distribution at a specified frequency. The technique selected for this purpose was the wavenumber-based version of the surface variational principle (SVP). One reason for selecting this approach was the manner in which it represents the surface response, which gives a physically meaningful picture. Specifically, it describes the surface dynamics in terms of waves on a two-dimensional sheet, which corresponds to the type of picture one would obtain from a nearfield acoustical holography experiment using meridional arclength as the aperture in the axial direction. The basis functions used to derive the surface impedance in this representation were also used to implement the frequency domain version of DAA. Thus, any differences in the solutions are solely a consequence of the difference in the manner in which the physical laws are modeled.

The problem selected for evaluation was a slender hemi-capped cylindrical shell whose cylindrical segment length  $2L$  is a factor of ten greater than the radius  $a$ , giving a tip-to-tip length to diameter ratio of  $2L/2a = 6$ . Because this work was intended to develop the basic methodology, only the axisymmetric aspects of the interaction model were addressed. The surface impedance matrix, whose elements represent the spectrum of pressure wavenumber amplitudes that are generated by a specific surface wave, was obtained by DAA and compared to that obtained from SVP. These comparisons were made for  $ka = 1, 4, 7$ , and  $10$ , which are values selected to be representative of the range associated with an explosive source. In addition to comparing the surface impedance directly, the alternative descriptions were also used to generate the response to a ring force. The DAA and SVP responses were compared for their content in the wavenumber space.

## 2. Research Approach

The basic concept of DAA is that the laws for interaction between a vibrating surface and the surrounding fluid are well understood in the limits of early-time, where the surface pressure is proportional to the surface normal velocity, and late-time, where the fluid reacts to the surface acceleration as an added-mass, as though the fluid were incompressible. DAA fits these limiting behaviors together in a manner that is suggested by the analytical solutions for spheres and infinitely

long cylinders [1], [2]. The analytical foundation for the project was the ability in linear vibrations and acoustics to transform between differential equations in the time domain, which is the manner in which DAA is usually implemented, and algebraic equations in the frequency domain, which is the manner used for most structural acoustics modeling techniques. In the frequency domain the relation between surface pressure and velocity variables may be written as

$$\mathbf{A}p = \mathbf{B}v, \quad (2.1)$$

where  $\mathbf{A}$  and  $\mathbf{B}$  are functions of frequency, which is nondimensionalized to  $ka$  and  $p$  and  $v$  are respectively nondimensionalized by  $\rho c^2$  and  $c$ . These dependencies, which are nonsingular, may be expanded in power series of  $ka$ , so that

$$\left[ \mathbf{A}_0 - ika\mathbf{A}_1 - (ka)^2 \mathbf{A}_2 \right] p = \left[ \mathbf{B}_0 - ika\mathbf{B}_1 - (ka)^2 \mathbf{B}_2 \right] v. \quad (2.2)$$

Note that the series are truncated at second order, corresponding to the DAA implementation, in which the differential equations are, at the most, second order in time. Also note that the coefficient matrices  $\mathbf{A}_j$  and  $\mathbf{B}_j$  are independent of  $ka$ .

A paper by Nicholas-Vuillierme [5] derived expressions for these matrices by expanding the surface Helmholtz integral in power series. For the low frequency region (late-time behavior) all surface response variable and the Green's function were expanded in powers of  $ka$ . Similar expansions in powers of  $1/ka$  were used to obtain the high frequency representation (early-time behavior). The general DAA representation between surface pressure and velocity variables obtained from these expansions is

$$\left[ \mathbf{I} - ika\mathbf{A}_1 - (ka)^2 \mathbf{A}_2 \right] p = \left[ -ika\mathbf{T}_0 - (ka)^2 \mathbf{A}_2 \right] v. \quad (2.3)$$

This form follows from the required asymptotic behavior. For example  $-ika\mathbf{T}_0v$  is the inertial resistance to acceleration presented by an incompressible fluid, while the identity of the highest order terms follows from the very high-frequency limit in which  $p$  and  $v$  are essentially equal because the rapidity of the fluctuation prevents distant locations from influencing the local interaction. Expressions for  $\mathbf{A}_1$  and  $\mathbf{A}_2$ , in the form of integrals over the surface area, were derived by Nicholas-Vuillierme; the integrands depend on the general manner in which the surface response is described. Different expressions for the  $\mathbf{A}_j$  arise depending on the level of approximation. The simplest version, usually referred to as DAA-1, requires evaluation of only  $\mathbf{A}_1$  and  $\mathbf{T}_0$ , which are different from the coefficients associated with DAA-2, in which all coefficients appearing in eq. (2.3) must be evaluated.

The research program began by evaluating via standard numerical methods the coefficients corresponding to the basis functions used to implement the wavenumber-based version of SVP. These coefficients are saved for subsequent use. This was done only for DAA-2, which logically should be the most accurate of the DAA approximations, and therefore give the best agreement with SVP. The corresponding surface impedance is obtained from

$$p = Z_{\text{daa}} v, \quad Z_{\text{daa}} = [\mathbf{I} - ika\mathbf{A}_1 - (ka)^2 \mathbf{A}_2]^{-1} [-ika\mathbf{T}_0 - (ka)^2 \mathbf{A}_2]. \quad (2.4)$$

The term  $\mathbf{T}_0$ , which represents the zero frequency added mass, was obtained according to the SVP technique, which is discussed below. Another program was written to evaluate  $Z_{\text{daa}}$  at specified frequencies as described above, and save the values.

Programs written prior to the commencement of the present project were run to determine and save the stiffness and mass matrices corresponding to an assumed modes analysis of the axisymmetric vibration of the shell. For the acoustic radiation problem used as the testbed for the methodology, the structural dynamic equations are

$$[\mathbf{K} - (ka)^2 \mathbf{M}] q = -\Lambda p + F \quad (2.5)$$

where  $q$  contains the coefficients of the series used to represent the displacement components of the shell,  $F$  is the corresponding set of generalized forces, and  $\Lambda$  is a coupling matrix mapping the pressure basis functions into the functions used to represent displacement. The fully coupled set of equations is obtained by assuring continuity of normal velocity at the wetted surface. This entails mapping the basis functions used to represent surface displacement into the wave functions used to represent surface velocity. The coefficients  $\Gamma$  that result from this operation are similar to, but usually different from, the coefficients  $\Lambda$ . The continuity condition leads to

$$v = -ika\Gamma q \quad (2.6)$$

It is straightforward to eliminate  $p$  and thereby obtain a set of simultaneous equations whose solution is the value of  $q$  at the specified frequency. Substitution of eq. (2.6) into the first of eqs. (2.4) leads to

$$p = -ikaZ_{\text{daa}}\Gamma q \quad (2.7)$$

which converts eq. (2.5) becomes

$$[\mathbf{K} - ika\Lambda Z_{\text{daa}}\Gamma - (ka)^2 \mathbf{M}] q = F \quad (2.8)$$

These formulation and solution of these equations were achieved by writing another program, which read the various matrices from disk storage and evaluated  $F$  corresponding to a ring force. (Recall that the investigation was limited to axisymmetric situations.)

The basis functions used to represent the surface pressure and shell displacements were the same as those used for the wavenumber version of SVP. These functions form half-range Fourier series whose type is selected to satisfy all continuity requirements at the apexes. These functions are taken to depend on the arclength  $s$  measured along the meridian from one apex, nondimensionalized by the total arclength  $s_0 = 2L + \pi a$ . The specific series expansions for the axisymmetric system are

$$\begin{aligned} p &= \sum_{j=1}^M P_j \cos\left(\frac{j\pi s}{s_0}\right) \\ w &= \sum_{j=1}^M W_j \cos\left(\frac{j\pi s}{s_0}\right), \quad u = \sum_{j=1}^M U_j \cos\left(\frac{j\pi s}{s_0}\right) \end{aligned} \quad (2.9)$$

where  $w$  and  $u$  are the displacement components of the shell normal and transverse to the wetted surface.

The values of  $Z_{\text{daa}}$  and  $q$  corresponding to DAA-2 were compared to those obtained from SVP using the same series expansions as eq. (2.9). The SVP surface impedance is given by

$$p = Z_{\text{svp}} v, \quad Z_{\text{svp}} = \mathbf{A}^{-1} \mathbf{B} \quad (2.10)$$

where  $\mathbf{A}$  and  $\mathbf{B}$  are the basic matrices derived by the wavenumber version of SVP. The evaluation of these coefficients entailed running a program previously developed by the Principal Investigator. Values of  $Z_{\text{svp}}$  and  $Z_{\text{daa}}$  at various frequencies were compared in color contour charts described in the next section. In addition,  $Z_{\text{svp}}$  was used as an alternative to  $Z_{\text{daa}}$  in the program that solved eq. (2.8). The structural responses predicted by DAA and SVP at each frequency were compared for wavenumber amplitudes.

It is important to recognize that the methodology employed in the research program represents a carefully controlled test. The same series representations of the surface pressure and surface velocity were employed to develop the DAA and SVP model equations. Furthermore, the added mass term used to form DAA (i.e. the zero frequency impedance) was identical to that given by SVP. In addition, the same

structural dynamic model was used in conjunction with the alternative fluid interaction laws. In fact, the evaluation of displacement was implemented by successive calls to the same subroutine, with one argument being the alternative surface impedances. It follows that any differences encountered between the two formulations are solely due to the approximations inherent in DAA.

### 3. Results

The example selected to test the research approach was a steel, hemi-capped cylinder whose cylindrical section is ten radii long, giving a total aspect ratio  $2L/2a = 6$ , measured tip to tip. The cylinder and caps were modeled as a shell capable of sustaining extensional and flexural deformation, with the thickness taken as  $a/50$ . In keeping with the exploratory nature of the work, no attempt was made to include the effects of internal ribs and substructures. The excitation was considered to be a ring force located at an axial distance of  $2.5a$  from the center, which corresponds to the one quarter point along the cylinder. Computations were performed for  $ka = 1, 4, 7$ , and  $10$ . The wavenumber spectrum was cutoff at  $M = 100$ , corresponding to wavelengths that are  $1/100$  of the cylinder's length. The adequacy of this truncation will be discussed.

To understand the results it is important to recognize a few fundamental aspects of the overall analysis.

- The results for the wet surface impedances are independent of the nature of the structure. These factors depend only on the shape of the wetted surface and the frequency. Thus, conclusions regarding these impedances apply to the axisymmetric response of any system having the model's shape.
- The degree to which the impedance factors influence the structural response depends strongly on the *in-vacuo* stiffness and inertia matrices, as is evident in eq. (2.8). Thus, conclusions drawn here as to the significance of modeling error associated with DAA should not be extrapolated to other structures, particularly, ribbed shells with internal structures.
- The example considered here exhibits left-right symmetry with respect to the transverse midplane. Thus, a surface velocity field exhibiting either symmetry or anti-symmetry will only excite a surface pressure having the same symmetry. Correspondingly, the surface impedance for symmetric

(even wavenumber) or antisymmetric (odd wavenumber) pressure distributions vanishes, respectively, for velocity distributions in the other symmetry group. For the sake of brevity, only the impedance factors associated with symmetric response will be discussed. The factors for antisymmetric response were found to behave in the same manner.

- The ring force excites both symmetric and antisymmetric wavenumbers, with the level of excitation of each being dependent on several factors. Consequently, differences between the even and odd wavenumber amplitudes is irrelevant to an assessment of the wavenumber distribution of the surface displacement.

The first set of figures are contours depicting the real and imaginary parts of the wet surface impedances. Figures 1 and 2 depict the real and imaginary parts of the impedance for  $ka = 1$ . According to both DAA and SVP, a surface velocity at a specified wavenumber primarily excites surface pressure waves at that and closely adjacent wavenumbers. These shall be referred to as self-impedances. The primary difference between SVP and DAA at this frequency is an underestimation of the peak real and imaginary values, although the overall patterns are very similar. Both analyses indicate that the real part of the self-impedances is cutoff, such that there is a transition from essentially real (resistive) to imaginary (inertial) self-impedance in the vicinity of wavelengths that are  $a/4$ . These effects become more evident as the frequency is increased in Figures 3-8. One can see that the contours predicted by SVP seem to scale upward with increasing  $ka$ . (Note the change in scale of the graph from  $ka = 1$  and 4 to  $ka = 7$  and 10.) The transition from resistive to inertial self-impedance predicted by SVP occurs sharply, and at an increasingly high wavenumber as the frequency is increased. This transition is much more gradual in the DAA results, and DAA fails to predict the peak self-impedance values. Furthermore, DAA fails to predict the highlights in the cross-impedances predicted by SVP in the vicinity of the cutoff. For the most part, the best agreement between DAA and SVP occurs in regions where the wavenumbers are much smaller or much larger than the cutoff wavenumber.

This cutoff phenomenon is recognizable as the transition from supersonic waves that radiate away from the surface to subsonic waves that evanesce off the surface. This feature will be explained later. In the region where the transition occurs SVP shows that the self-impedances rise rapidly, and then suddenly transition to a large inertial value that then progressively decreases with decreasing wavelength. Both parts of the cross-impedances (pressure amplitudes induced by surface waves

at other wave numbers) fluctuate rapidly in all directions in the vicinity of this transition. This is contrasted with the predictions obtained by DAA, which fails to show a sharp transition from resistive to inertial impedance, and correspondingly fails to predict the peak impedance values in the vicinity of the transition.

A simple demonstration that the highlights of the surface impedance correspond to a transition from supersonic to subsonic waves is available. Because the response is axisymmetric, surface waves propagate in the meridional direction only. The total distance along the meridian for a wave to return to its starting point is  $s_{\text{tot}} = 2(2L + \pi a)$ . The wavelength of a sonic wave (phase speed equal to the speed of sound) is  $\lambda = 2\pi/k$ , so the number of such waves lying along the closed meridional path is  $N = s_{\text{tot}}/\lambda = ka(L/\pi a + 1)$ . This leads to  $N = 4, 17, 29,$  and  $42$  at  $ka = 1, 4, 7,$  and  $10$ , respectively. In contrast, the peak real impedance occurs in the SVP results at  $N = 4, 17, 29,$  and  $42$  in the corresponding Figures 1, 3, 5, and 7. (The minor discrepancies in these values of  $N$  are consequences of considering the surface impedances for symmetric responses relative to the midplane, which limits the wavenumbers in the figures to even values.)

Figures 10 to 13 describe the surface displacement at the four frequencies of the example; Figure 9 depicts the quasistatic ( $ka \approx 0$ ) response. These results are depicted as the amplitude of the displacement wave at each wavenumber. Both the normal ( $W$ ) and in-plane ( $U$ ) displacements are shown for completeness, but it is clear that the transverse motion is dominant at all frequencies. Note that the amplitudes attain a peak value with increasing wavenumber, and then fall off rapidly. In the case of  $ka = 10$ , this fall off occurs in the vicinity of the highest wavenumber retained in the analysis, which suggests that this computation should be redone retaining more waves. Except for  $ka = 4$ , the DAA and SVP predictions agree closely, with the largest disagreement occurring at the portion of the wavenumber spectrum where the amplitudes peak. In the case of  $ka = 4$  the amplitudes are significantly larger than at the other frequencies, which suggests that this frequency is close to a submerged resonance. The strong disagreement between the DAA and SVP predictions for this frequency might be a breakdown of DAA, but it is more likely that it stems from a slight misprediction of the frequency at which the resonance occurs. One would need to perform a reasonably fine frequency sweep to identify which is the cause for the discrepancies.

## 4. Conclusions

This project successfully developed a methodology for testing the accuracy of DAA in modeling fluid-structure interaction for realistically shaped submerged structures. The approach uses the frequency-domain equivalent of the time-domain DAA differential equations, and then compares it to results obtained from a standard structural acoustics approach of known accuracy. Each method is used to construct alternative surface impedance matrices corresponding to a specified set of basis functions for surface velocity and pressure. These alternative predictions were compared directly, and also used as alternative inputs representing the fluid loading effects for an acoustic radiation problem. Consistent with the formative nature of the research, only axisymmetric situations were considered.

The results for a reasonably long hemi-capped cylindrical shell disclosed that DAA fails to properly predict the transition from supersonic to subsonic waves as the wavelength decreases. This failure is not surprising. In fact, it points to a rather obvious failure of the logic behind DAA. One fundamental physical argument underlying DAA is the statement that at a sufficiently high frequency, the impedance is a local and primarily planar. Such a statement ignores the fundamental fact that **at any frequency there is a wavelength below which the wave is subsonic and evanesces away from the surface.** The behavior of these short waves does not resemble the resistive nature of a planar wave.

The predictions for surface motion obtained from DAA agreed well with the structural acoustics computation at three frequencies. Its failure at the fourth frequency might be attributable to a small error in predicting the frequency of a fluid-loaded resonance. Further investigation in the form of a fine frequency sweep would be required to identify definitively the cause of the discrepancy. The present results indicate that, for the ideal model addressed in the research program, DAA is more accurate for predicting structural displacement than it is for predicting the pressure waves induced by the displacement.

It is important to recognize that the foregoing conclusions regarding the accuracy with which DAA predicts surface impedance is general, because the analysis of that aspect is independent of the nature of the structure. In contrast, there is no way to ascertain without considering other, more realistic, models whether the conclusions regarding the ability of DAA to predict structural motion are generally valid.

## References

- [1] T. L. Geers, "Residual potential and approximate methods for three-dimensional fluid-structure interaction problems," *Journal of the Acoustical Society of America*, vol. 49, 1505-1510 (1971).
- [2] T. L. Geers, "Doubly asymptotic approximations for transient motion of submerged structures," *Journal of the Acoustical Society of America*, vol. 64 1500-1508 (1978).
- [3] J. W. Wawa and F. L. Dimaggio, "Dynamic response of a submerged prolate spheroidal shell to a longitudinal shock wave," *Computers and Structures*, vol. 20, 975-989 (1985).
- [4] L. G. Olson and K.-J. Bathe, "An infinite element for transient fluid-structure interactions," *Engineering Computation*, vol. 2, 319-329 (1985).
- [5] B. Nicholas-Vuillierme, "A contribution to doubly asymptotic approximations: an operator top-down derivation," *Numerical Techniques in Acoustic Radiation*, R. J. Bernhard and R. F. Keltie, eds, ASME-NCA Vol. 6, 7-13 (1989).

# Wet Surface Impedance Symmetric Terms, $ka = 1$

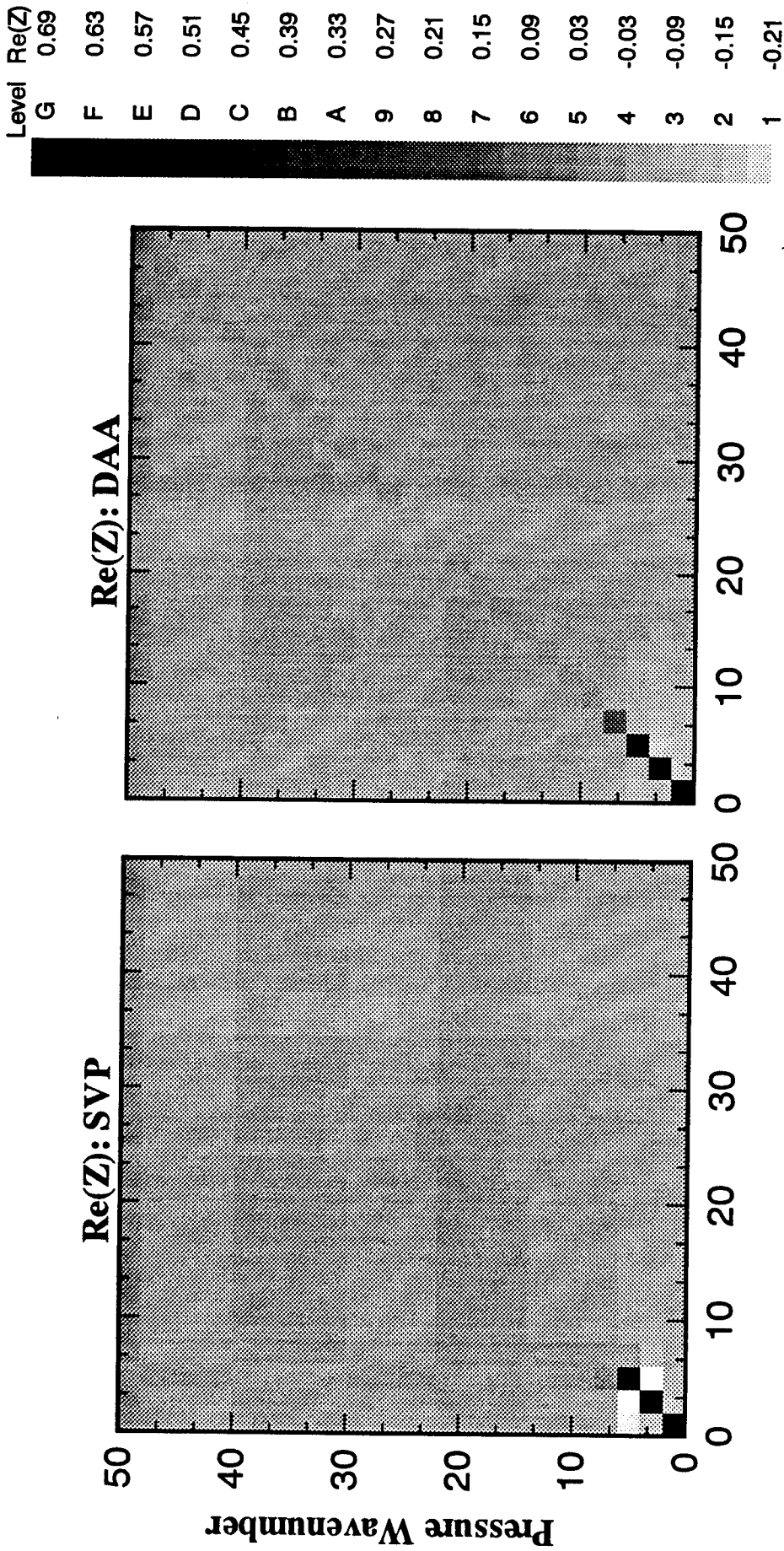


**Figure 1**

# Wet Surface Impedance Symmetric Terms, $ka = 1$

Level	$\text{Im}(Z)$
F	0.20
E	0.12
D	0.04
C	-0.04
B	-0.12
A	-0.20
9	-0.28
8	-0.36
7	-0.44
6	-0.52
5	-0.60
4	-0.68
3	-0.76
2	-0.84
1	-0.92

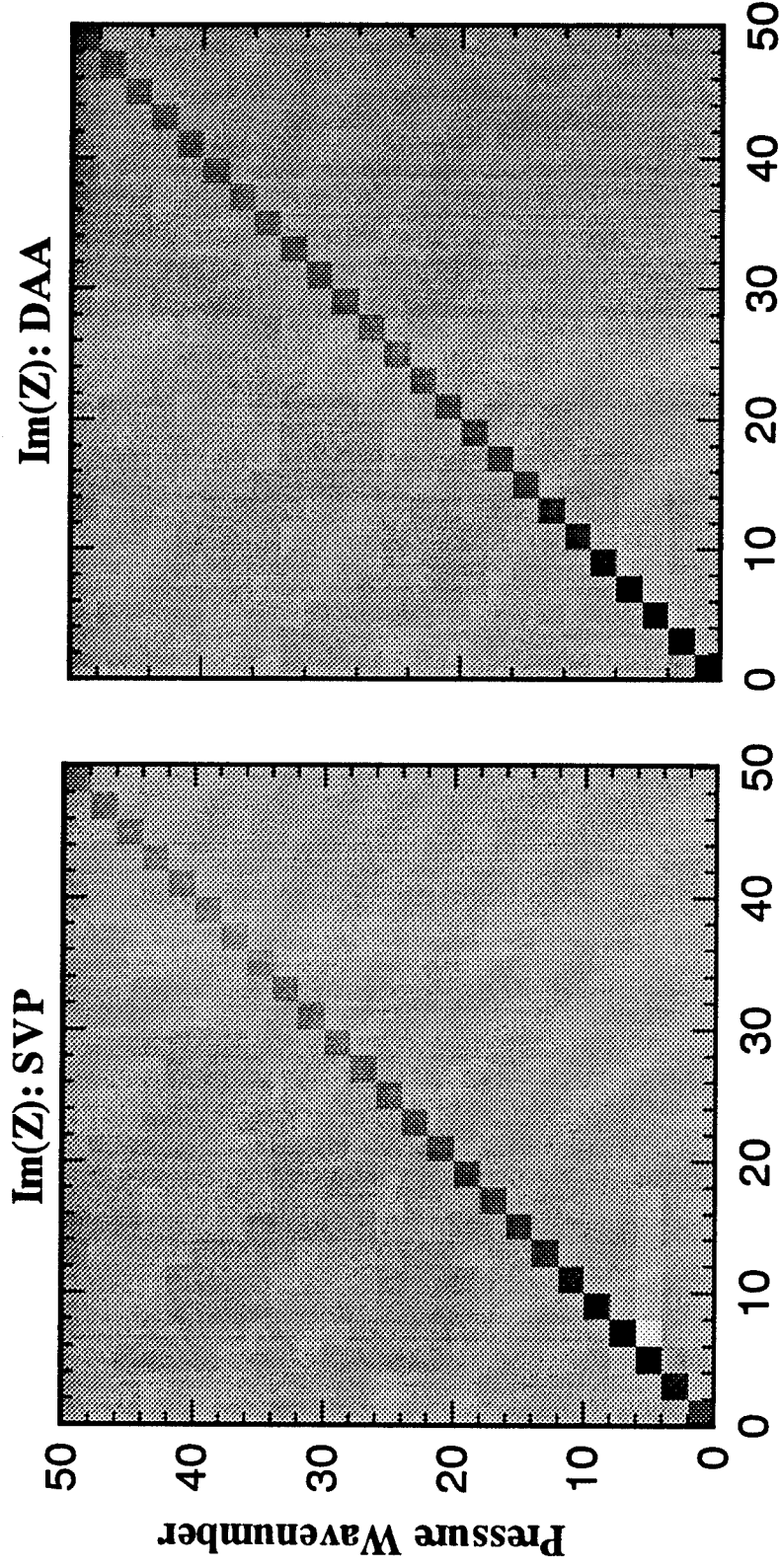


**Figure 2**

# Wet Surface Impedance Symmetric Terms, $ka = 4$

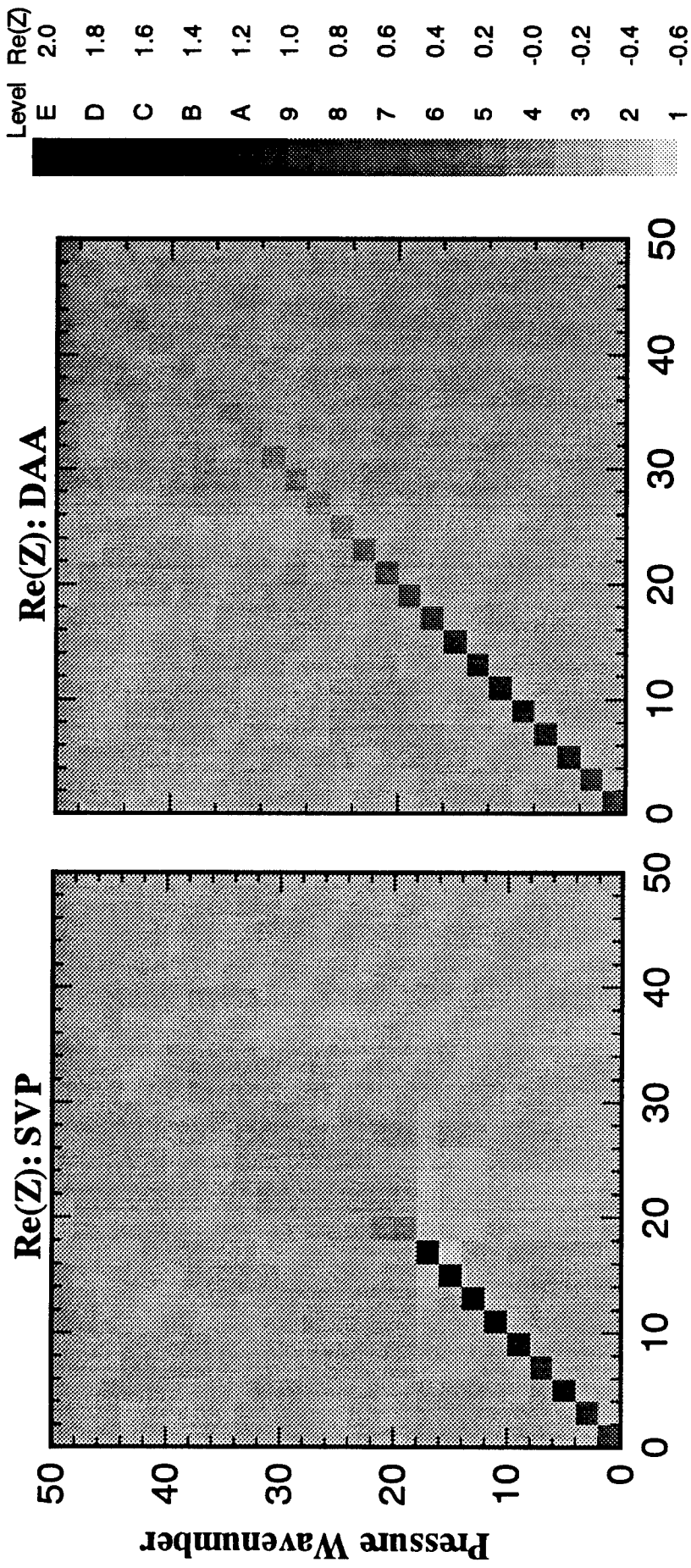
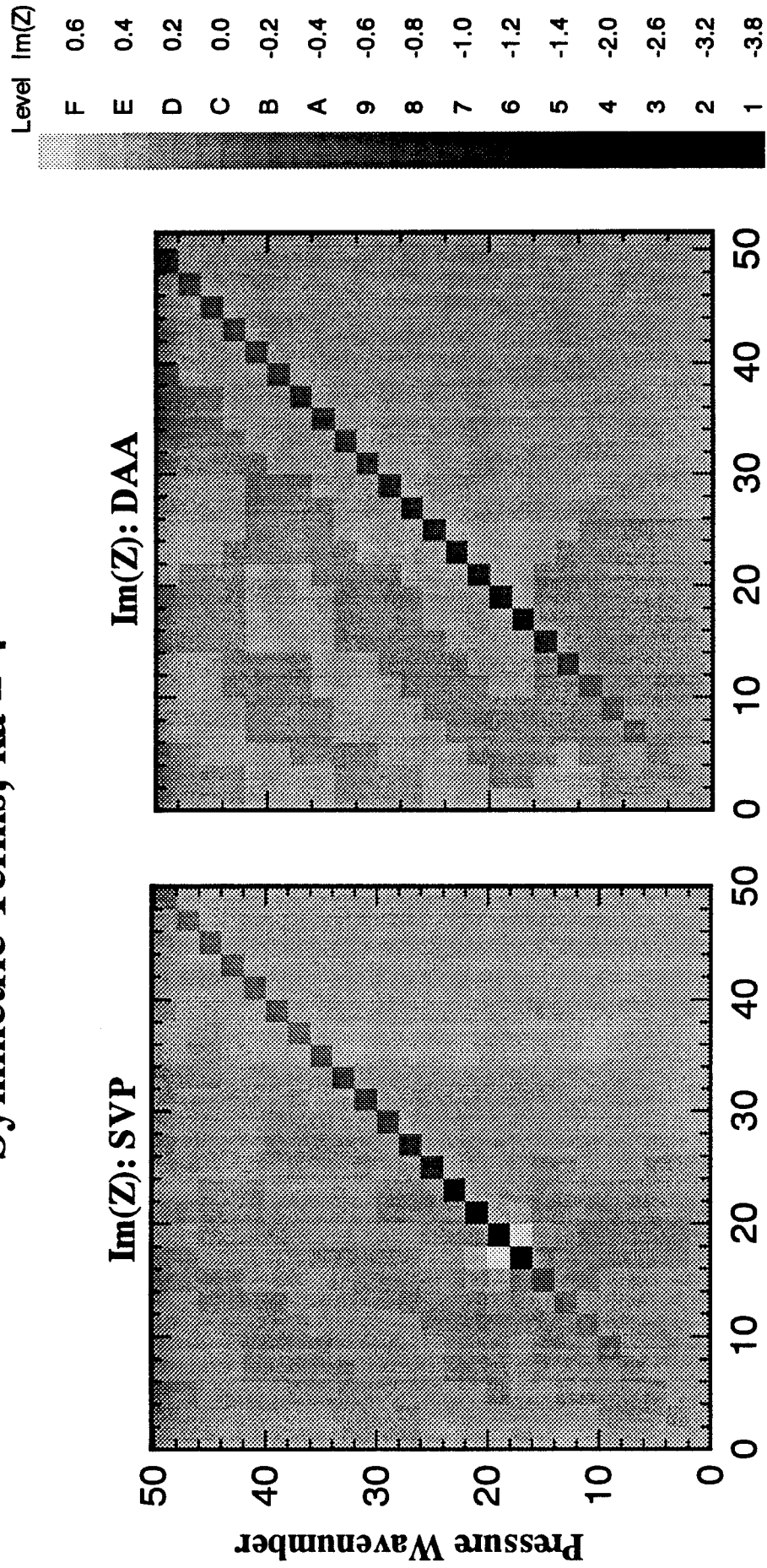


Figure 3

# Wet Surface Impedance Symmetric Terms, $ka = 4$



**Figure 4**

**Wet Surface Impedance  
Symmetric Terms,  $ka = 7$**

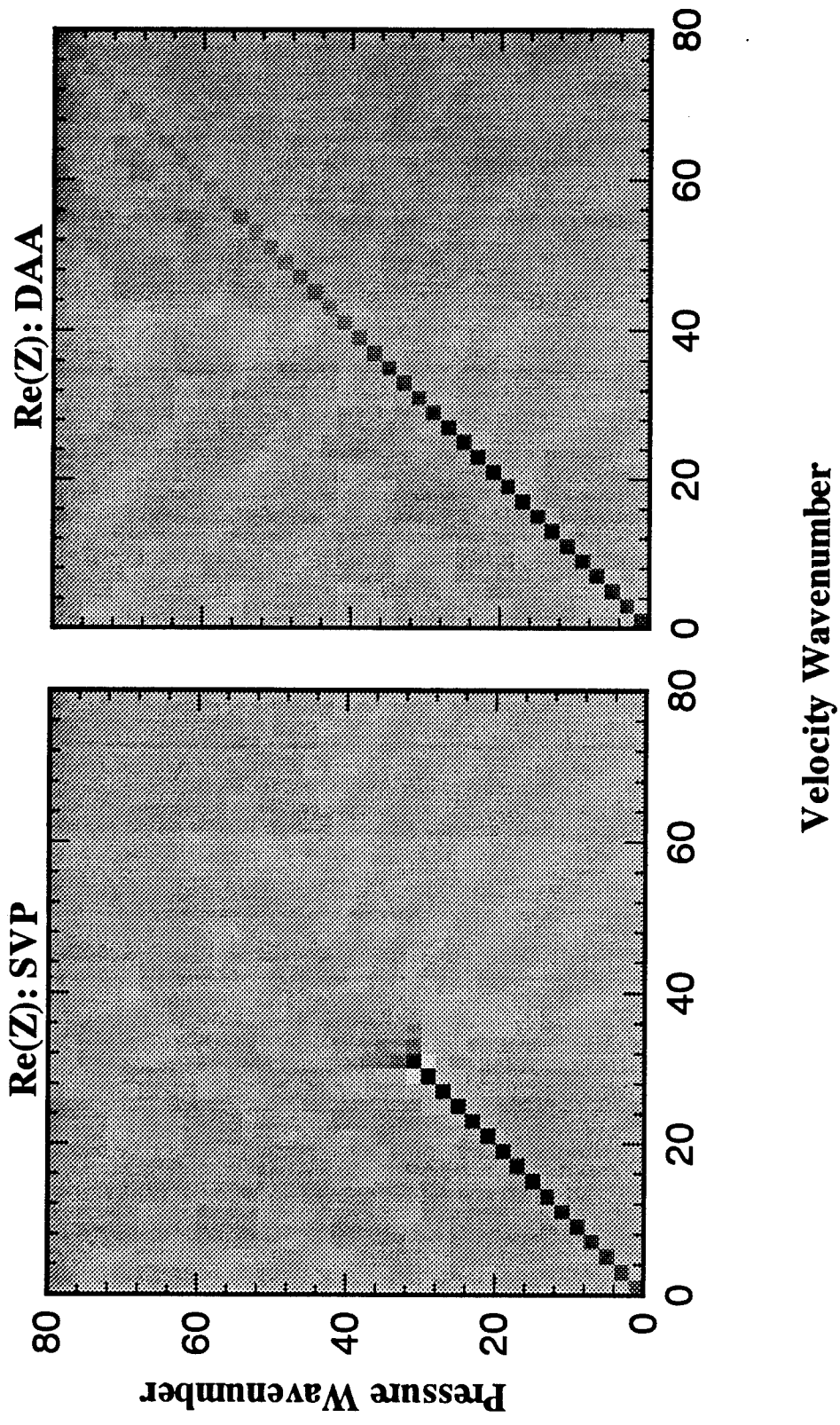


**Figure 5**

# Wet Surface Impedance Symmetric Terms, $ka = 7$

Level	$\text{Im}(Z)$
F	0.6
E	0.4
D	0.2
C	0.0
B	-0.2
A	-0.4
9	-0.6
8	-0.8
7	-1.0
6	-1.2
5	-1.4
4	-2.0
3	-2.6
2	-3.2
1	-3.8

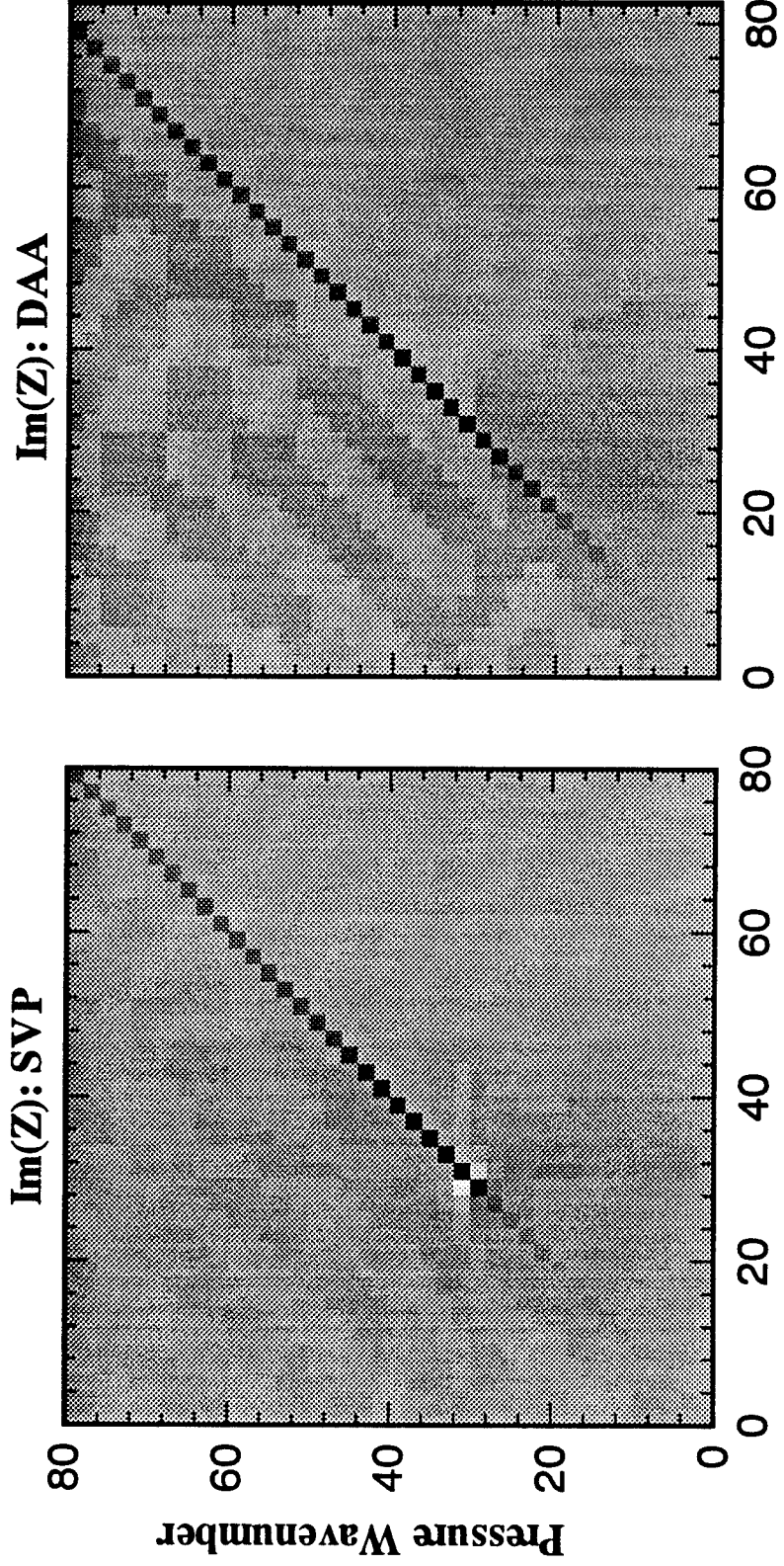


**Figure 6**

# Wet Surface Impedance Symmetric Terms, $ka = 10$

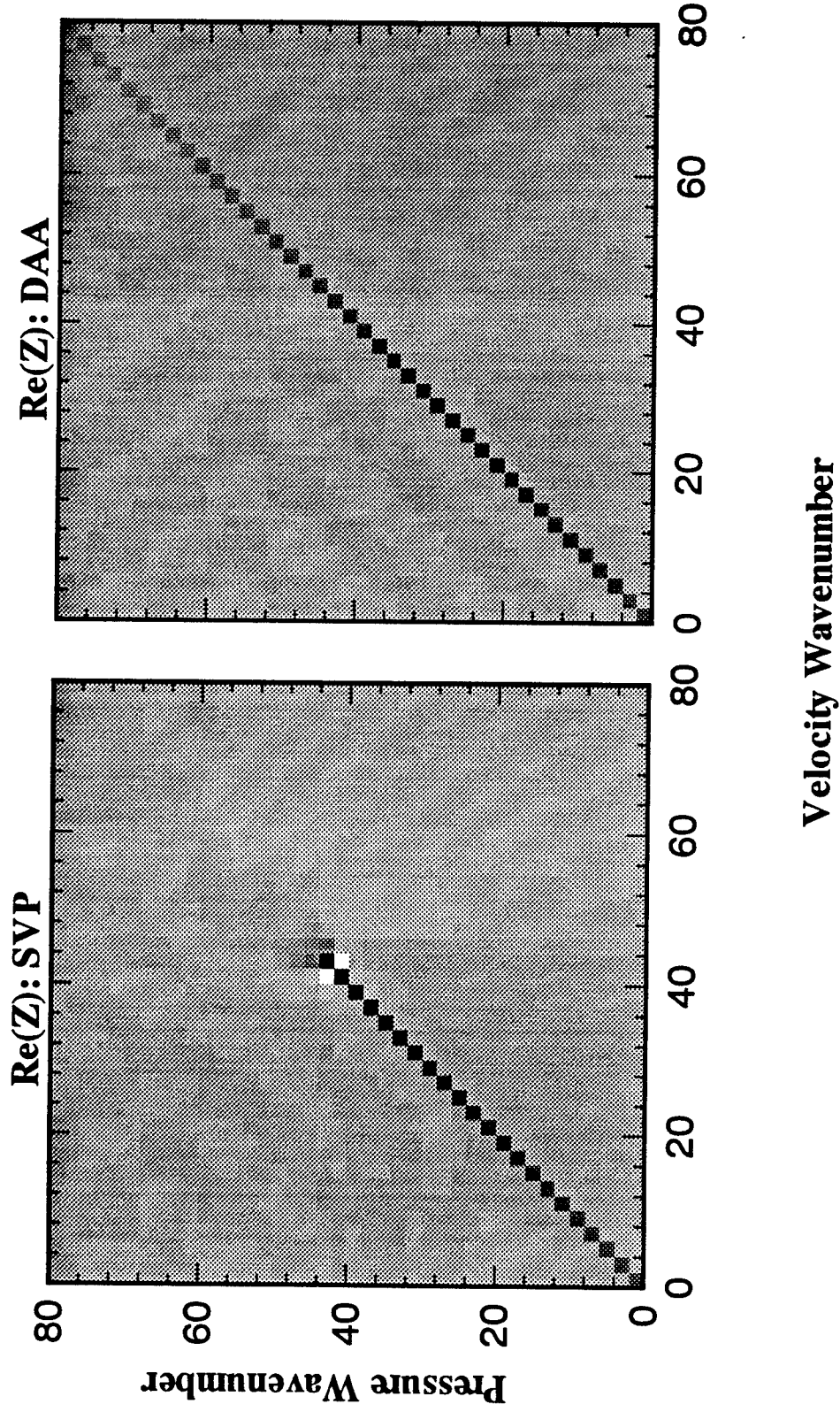
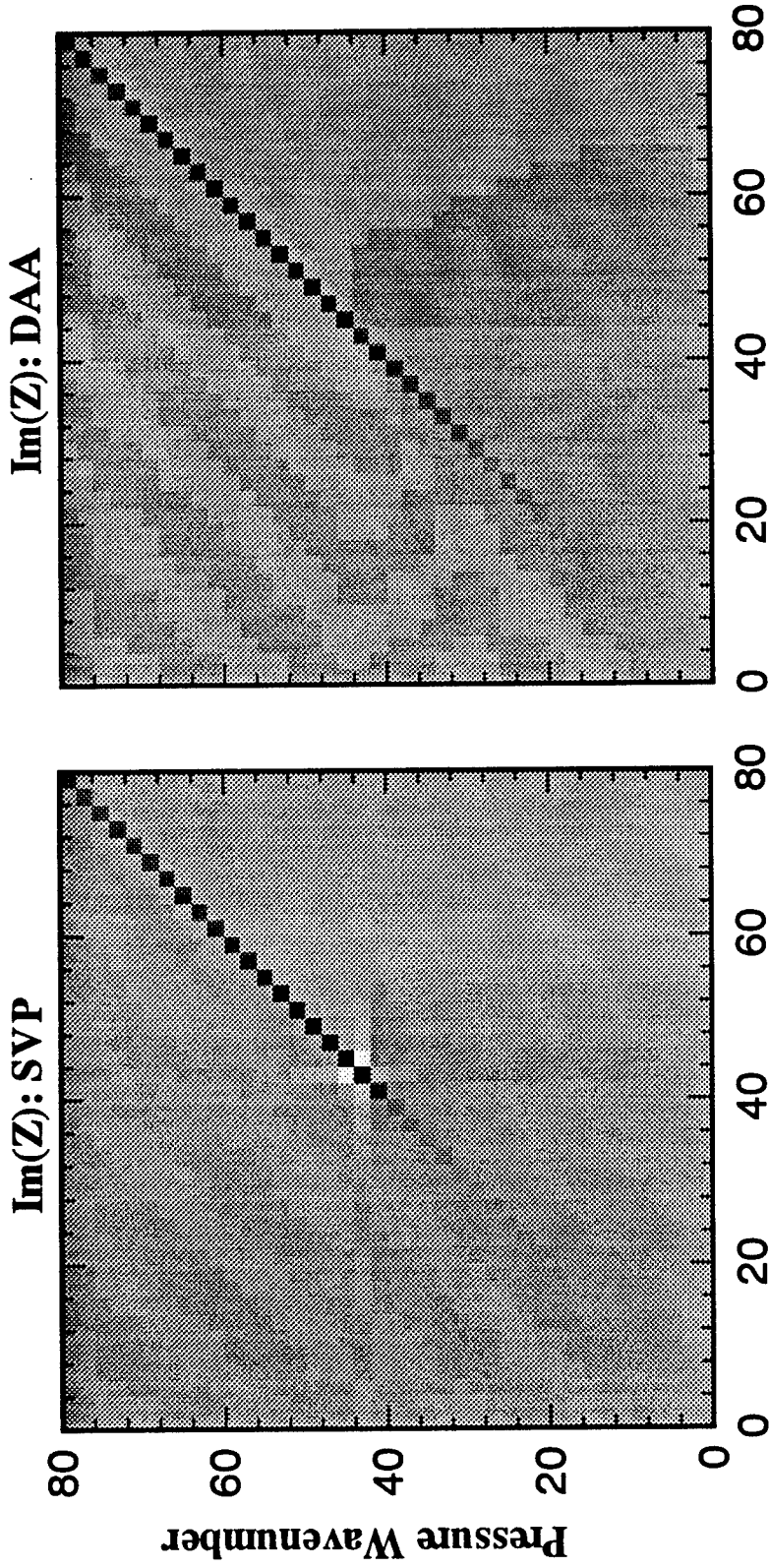


**Figure 7**

**Wet Surface Impedance  
Symmetric Terms,  $ka = 10$**

Level	$\text{Im}(Z)$
F	0.6
E	0.4
D	0.2
C	0.0
B	-0.2
A	-0.4
9	-0.6
8	-0.8
7	-1.0
6	-1.2
5	-1.4
4	-2.0
3	-2.6
2	-3.2
1	-3.8



Velocity Wavenumber

**Figure 8**

Amplitudes,  $ka=0$ , ring force at  $z/a=2.5$

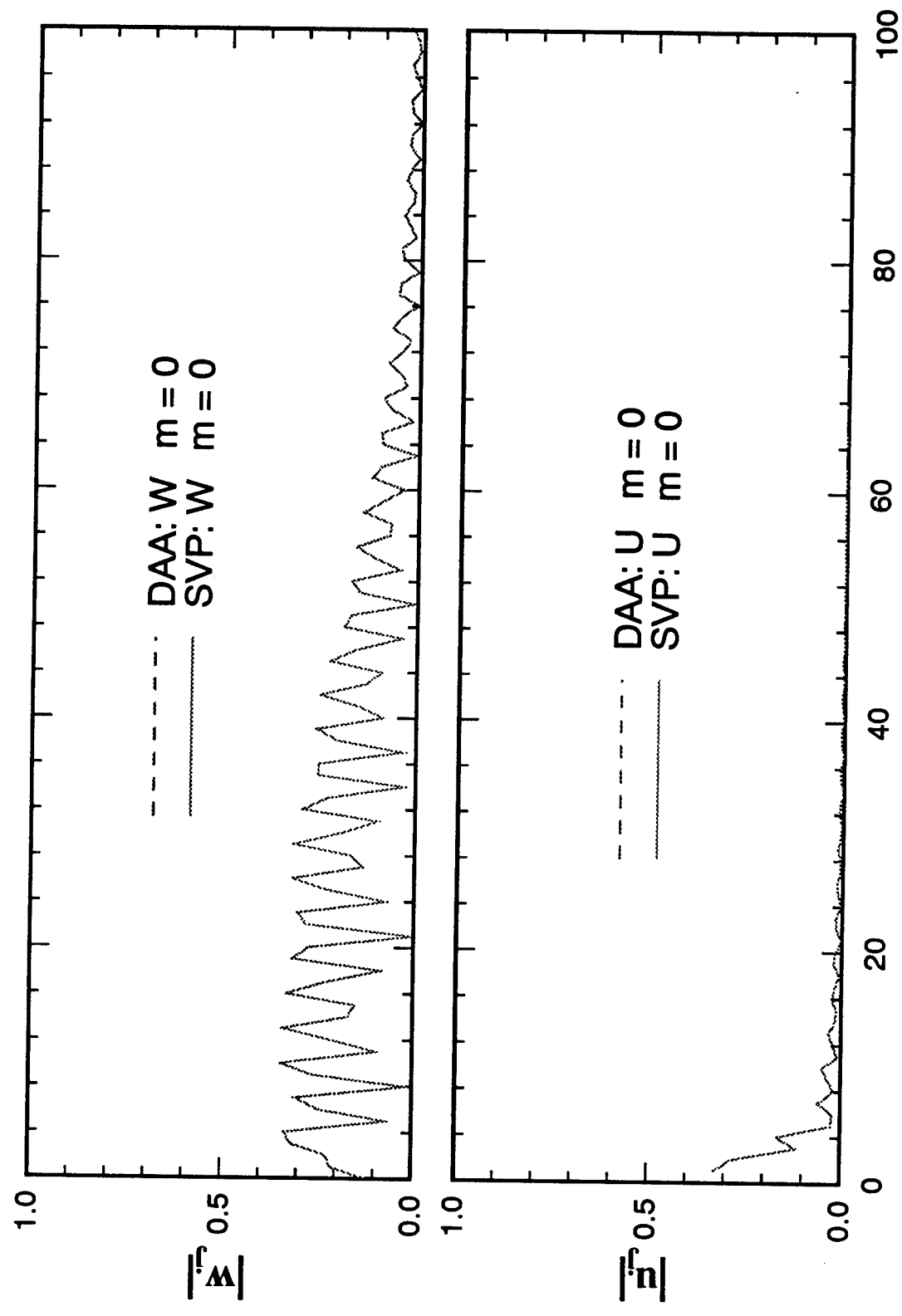


Figure 9

Amplitudes,  $ka=1$ , ring force at  $z/a=2.5$

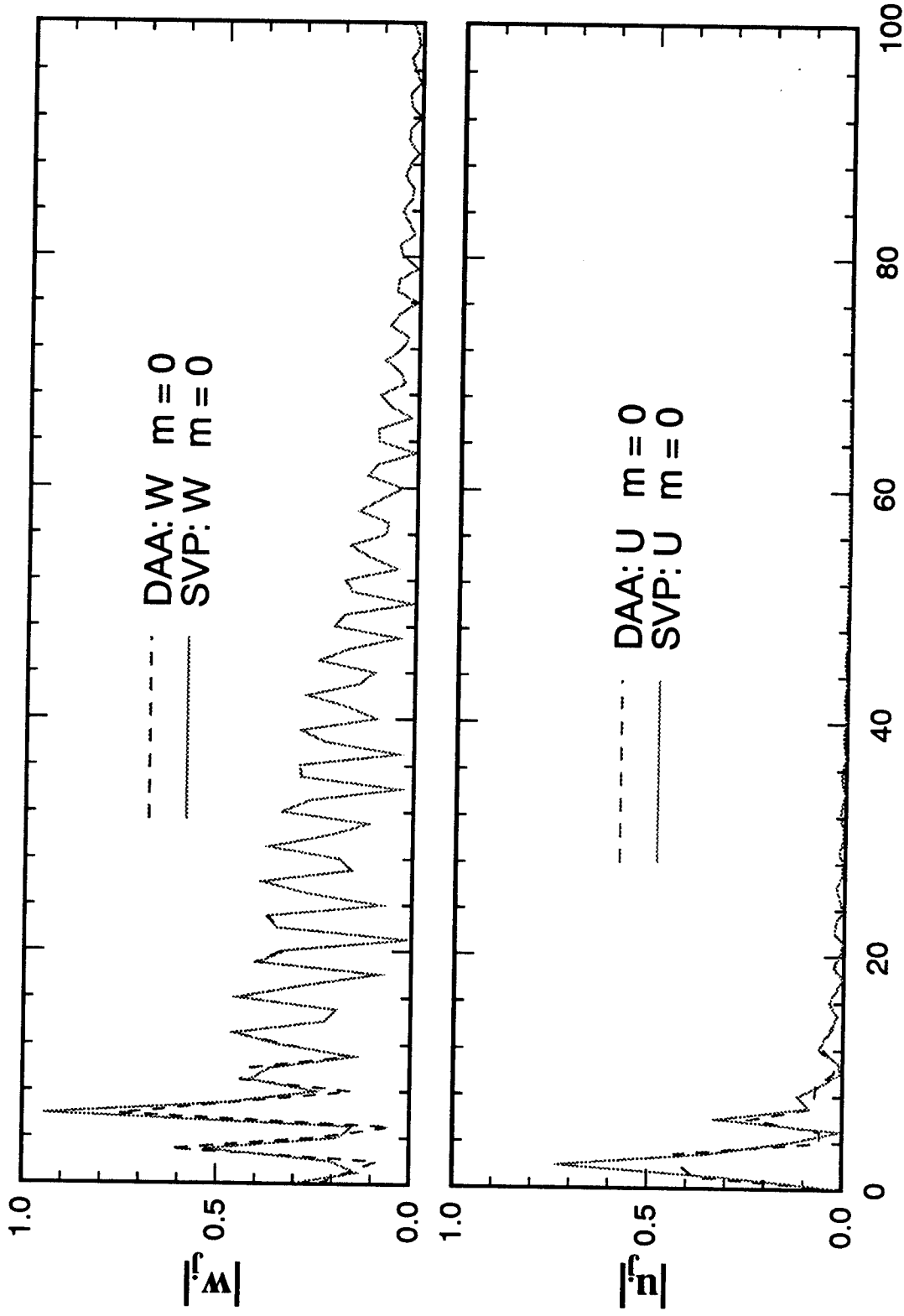


Figure 10

Amplitudes,  $ka=4$ , ring force at  $z/a=2.5$

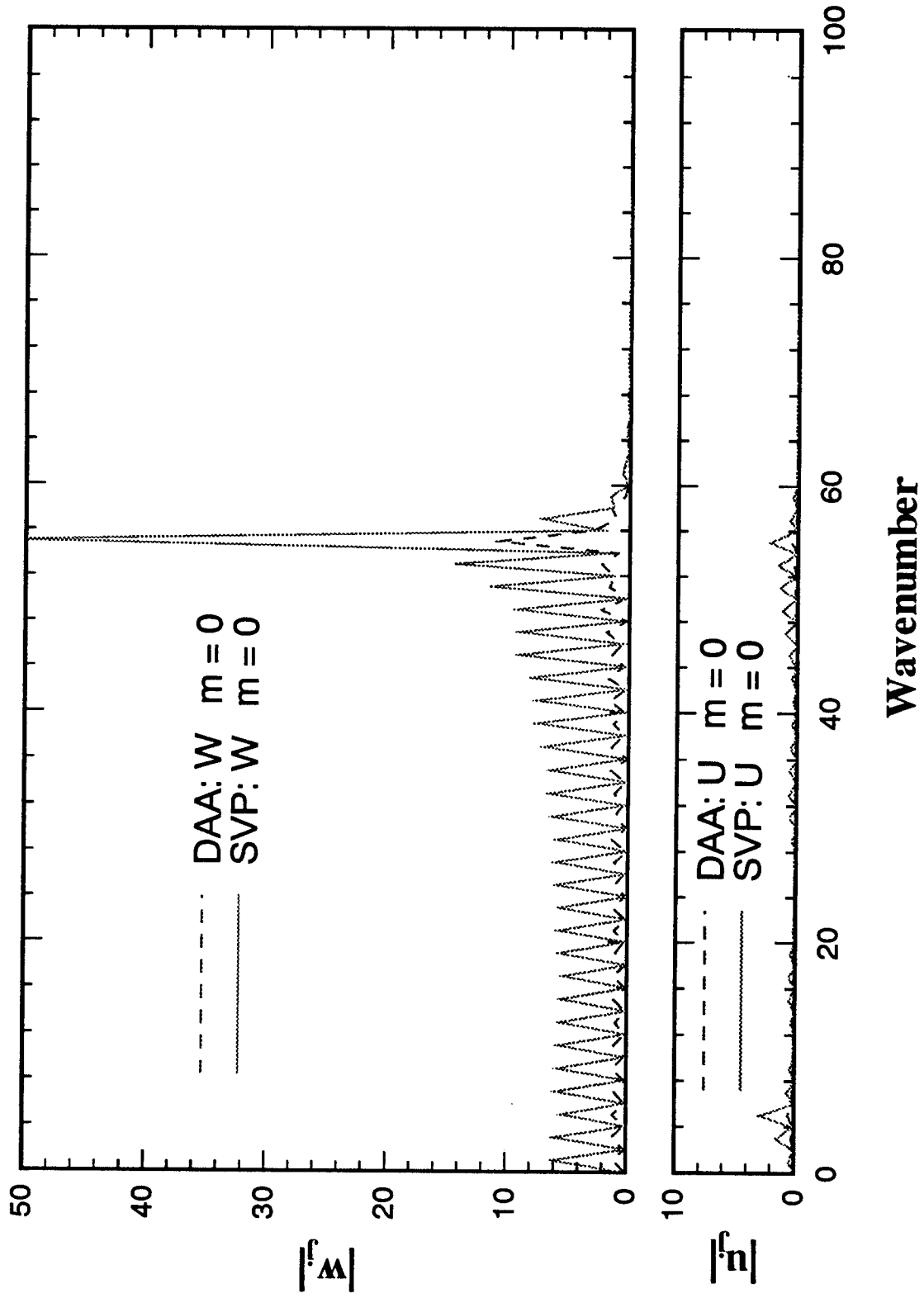


Figure 11

# Amplitudes, $ka=7$ , ring force at $z/a=2.5$

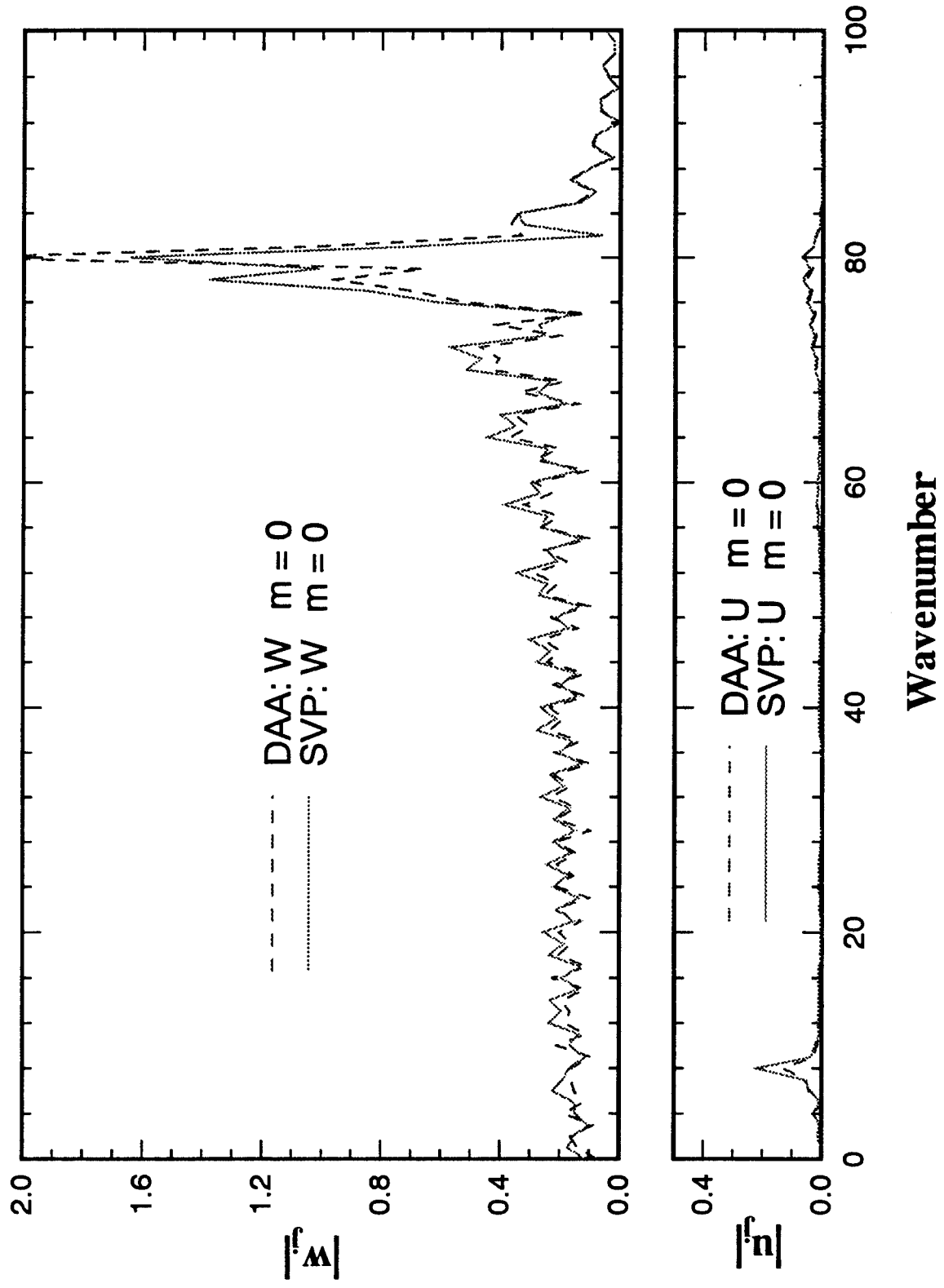
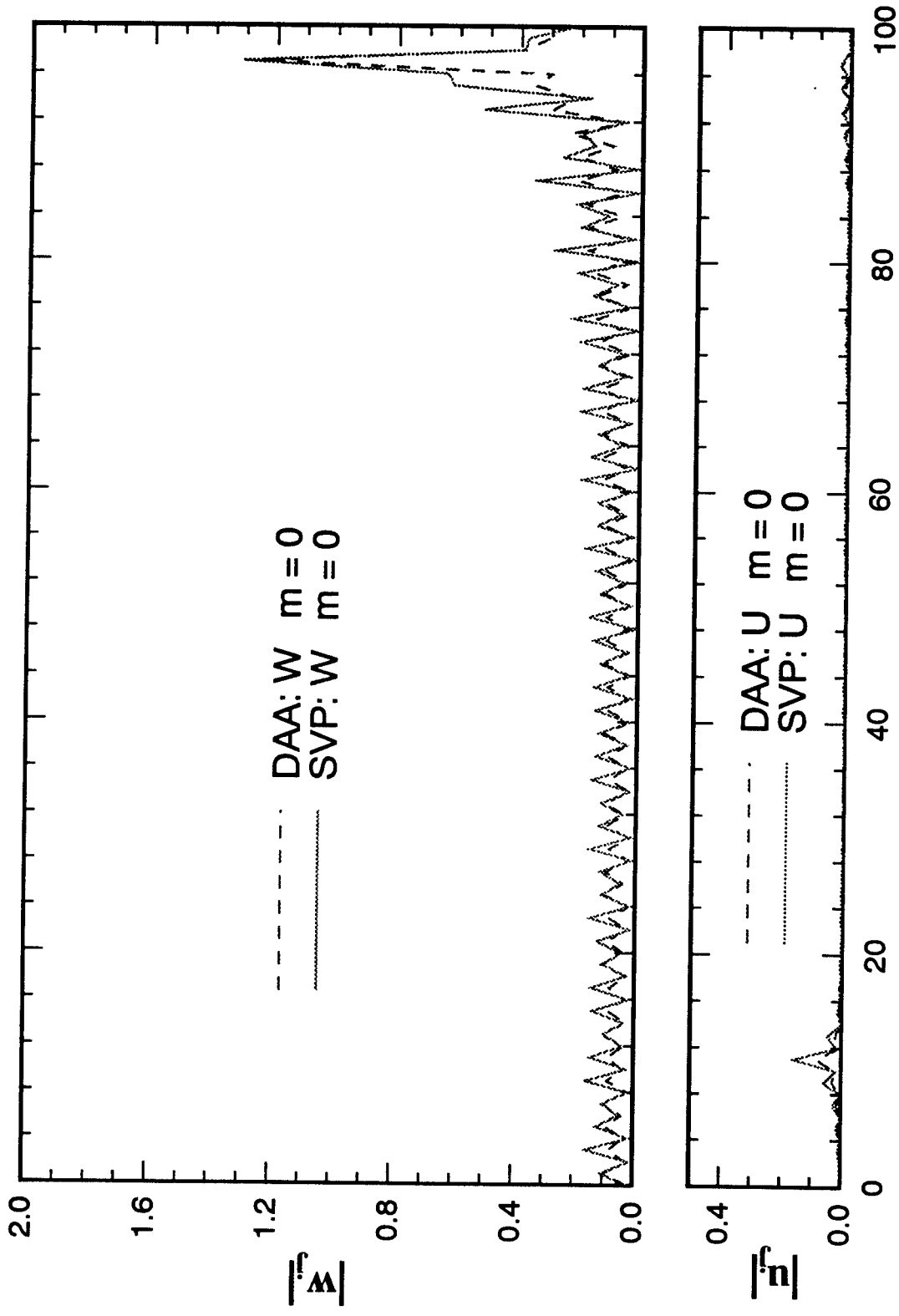


Figure 12

Amplitudes,  $ka=10$ , ring force at  $z/a=2.5$



Wavenumber

Figure 13